FINAL TASK REPORT

(AFOSR Contract F49620-03-C-0045)

Instructions: Provide all information identified below for the last FY only. List Research Objectives in bullet format. Provide Summary of Progress and Forecast for next FY in narrative format.

Research Title: Correlative Dynamics Studies Using the Weber Sodium Lidar and Associated Instrumentation at the ALOMAR Observatory

Principal Investigator: Dr. David C. Fritts NWRA/CoRA
Co-Principal Investigator: Prof. Chao-Yao She, CSU/Physics

Commercial Phone: 303-415-9701 FAX: 303-415-9702

Mailing Address: Colorado Research Associates /NorthWest Research Associates, Inc.

3380 Mitchell Lane

Boulder, Colorado 80301

E-Mail Address: dave@cora.nwra.com

AFOSR Program Manager: Major David Byers

Research Objectives:

1. Define the mean and variable structure of the MLT

Our objective here was to define the seasonal, inter-annual, and shorter-term variability of the thermal and wind structures throughout the mesosphere and lower thermosphere (MLT). Some of the relevant questions motivating this study include 1) why is the fall transition (increasing mesopause temperature during August) faster than the spring transition, 2) what are the corresponding mean winds and gravity wave momentum fluxes that account for these differences, 3) why is the summer mesopause temperature so stable (or is it?), 4) what is the morphology of mesospheric inversion layers, are there diurnal variations, and how do they depend on gravity wave forcing, and 5) are the strong shears in the lower thermosphere the source of, or the response to, gravity wave instability and momentum transport? These topics were addressed with long-term measurements of the thermal and wind fields over as full a range of altitudes as the Weber lidar and other ALOMAR instrumentation permit (typically ~10 to 105 km for both winds and temperatures). Though full-column measurements were only possible during comprehensive measurement campaigns, Weber lidar measurements spanned a much greater range of times throughout the years of operation.

2. Define the gravity wave coupling from lower altitudes

REPORT DOCUMENTATION PAGE

Form Approved
OMB No. 0704-0188

1. REPORT DATE *(DD-MM-YYYY)*	**2. REPORT TYPE**	**3. DATES COVERED** *(From - To)*
31-03-2006	Final Report	8/1/03 – 12/31/05

4. TITLE AND SUBTITLE

Correlative Dynamics Studies Using the Weber Sodium Lidar and Associated Instrumentation at the ALOMAR Observatory

5a. CONTRACT NUMBER
F49620-03-C-0045

5b. GRANT NUMBER

5c. PROGRAM ELEMENT NUMBER

6. AUTHOR(S)

Dr. David Fritts

5d. PROJECT NUMBER

5e. TASK NUMBER

5f. WORK UNIT NUMBER

7. PERFORMING ORGANIZATION NAME(S) AND ADDRESS(ES)

NorthWest Research Associates
14508 NE 20th St.
PO Box 3027
Bellevue, WA 98009-3027

8. PERFORMING ORGANIZATION REPORT NUMBER
NWRA-BELL-06-R320

9. SPONSORING / MONITORING AGENCY NAME(S) AND ADDRESS(ES)
Air Force Office of Scientific Research
AFOSR/NM Attn: Major David L. Byers
4015 Wilson Blvd., Rm. 713
Arlington, VA 22203 - 1954

10. SPONSOR/MONITOR'S ACRONYM(S)

11. SPONSOR/MONITOR'S REPORT NUMBER(S)
AFRL-SR-AR-TR-06-0153

12. DISTRIBUTION / AVAILABILITY STATEMENT

Distribution Statement A: Approved for Public Release

13. SUPPLEMENTARY NOTES

14. ABSTRACT

This contract supported continuing use of the Weber lidar for dynamics studies in the mesosphere, thermosphere, and ionosphere. The system performed well at the onset of this research, but we spent some resources on continuing improvements in the stability and "user-friendliness". Major measurement efforts during the summer 2002 and winter 2003 MaCWAVE rocket and ground-based measurement campaigns yielded extensive data sets that consumed the majority of our analysis resources. Results revealed a highly active and variable summer mesopause environment, with large wave amplitudes, extreme temperature and wind gradients, strong turbulence and mixing, and pronounced differences from previous or following years. It was determined that these differences arose from unusual planetary wave forcing prior to the southern hemisphere stratospheric warming having dynamical influences at high northern latitudes! Winter data revealed a similarly active environment exhibiting strong tidal motions, gravity wave filtering by mean winds, and strong temporal variability. Related theoretical efforts contributed a new, complete dispersion relation that allows computation of wave influences to very high altitudes and an assessment of solar influences on these dynamics. We expect our results to be especially relevant to AFOSR interests in wave coupling to altitudes well into the thermosphere and ionosphere.

15. SUBJECT TERMS

16. SECURITY CLASSIFICATION OF:			**17. LIMITATION OF ABSTRACT**	**18. NUMBER OF PAGES**	**19a. NAME OF RESPONSIBLE PERSON**
a. REPORT	**b. ABSTRACT**	**c. THIS PAGE**			**19b. TELEPHONE NUMBER** *(include area code)*

Gravity wave coupling studies require both 1) a description of the mean and variable thermal and wind fields through which the waves propagate (objective 1) and 2) as complete a quantification of the dominant wave structures at each altitude as possible.
Our research focused on definition of gravity wave amplitudes, vertical scales, directionality, and momentum fluxes through correlative measurements employing the Weber lidar and other ALOMAR instrumentation. Analyses of our various data sets focused on wave propagation and momentum transport.

3. Defining the important wave-wave and wave-mean flow interactions

Wave-wave interactions are largely responsible for gravity wave momentum flux modulation and for the spectral evolution of the wave field in the MLT. Wave-mean flow interactions require sensitivity to both the local mean flow and the waves (primarily gravity waves) accounting for the momentum fluxes and flux divergences at these altitudes. Measurements throughout the full cycle of the dominant modulations are required and were performed using the Weber lidar and the ALOMAR MF and meteor radars.

4. Gravity wave instability dynamics and effects

Detailed observational studies of gravity wave instability dynamics are perhaps the most challenging of those proposed in this effort. To address this need, we combined quantification of the gravity wave field (scales, amplitudes, and momentum fluxes) with the Weber lidar with mean wind measurements by various radars and optical definition of smaller-scale structures that arise from instability processes. This in situ sensitivity to small-scale structure and turbulence was made possible during the correlative MaCWAVE/MIDAS rocket, lidar, and radar campaign and led to such determinations.

Funding Summary, September 2004 to August 2005:

In House	Capital Equip. (> $5,000 each)	Subcontractor	Total
$322,044		$184,956	$506,000

Summary of Progress:

The Weber sodium lidar was constructed under a Defense University Research Instrumentation Program (DURIP) award to Colorado State University (CSU) and installed at ALOMAR (Arctic Lidar Observatory for Middle Atmosphere Research) in August 2000. Technical and scientific progress with the Weber lidar, from its installation until August 2003, was supported by a research contract to NorthWest Research Associates, Colorado Research Associates Division (NWRA/CoRA), and CSU under AFOSR funding (contract F49620-00-C-0008) and was described in the reports accompanying that contract. Here we report only on activities under the present contract. Significant scientific advances were made possible by this and supplemental funding for lidar operations and rocket campaign support from NSF and NASA.

a. Technical Progress

Improved stability was achieved with the sum-frequency generation (SFG) seeder late in 2004, and further enhancements to this system were implemented in 2005. The SFG has now performed very well in a number of measurement programs and a variety of conditions, and it can now be operated by colleagues in Norway having relatively little system expertise. Indeed, the SFG success with the Weber lidar at ALOMAR has prompted Prof. She to implement the same SFG technology in his lidar system at CSU in Fort Collins.

b. Scientific Progress

Significant aspects of all four research objectives listed above were addressed through a combination of collaborative measurement programs and analyses. Further efforts with data collected during the comprehensive Mountain and Convective Waves Ascending Vertically (MaCWAVE) and MIDAS rocket and ground-based measurement programs defined the unusual aspects and variability during our winter 2003 measurements. A more recent campaign (DELTA, December 2004) was performed by Japanese colleagues, and these results likewise yielded interesting insights into MLT structure and variability. In each case, the Weber lidar contributed in a major way to the measurement program. Indeed, it was the primary reason for proposing to perform both rocket campaigns at the Andoya Rocket Range (ARR) adjacent to ALOMAR. The summer 2002 and winter 2003 data sets have proven to be by far the most comprehensive data sets available on the MLT under polar mesopause conditions. Nevertheless, other measurements with the Weber lidar alone have proven valuable in addressing gravity wave momentum fluxes and their modulation through wave-wave interactions with the larger-scale motion field. Below, we highlight the results obtained with the Weber lidar and the implications of the science enabled by our correlative measurements throughout this research support.

1. Dynamics of the summer polar atmosphere

Our research goals with the Weber lidar were addressed, under summer conditions, primarily through measurements occurring as part of the comprehensive summer MaCWAVE rocket and ground-based measurement program performed at ARR and ALOMAR to define and quantify the gravity wave (GW) forcing, interactions, and instability processes accounting for the summer mesopause thermal, wind, and constituent structure in a manner not possible at any other location. This program included two ~12-hr rocket salvoes (a total of 26 MET rockets and 5 sounding rockets) launched on 1/2 and 4/5 July 2002 during intervals of clear weather and active PMSE, allowing us to take advantage fully of correlative instrumentation at ALOMAR, and especially the Weber resonance and Rayleigh lidars. Additional correlative measurements of MLT temperatures and turbulence fluctuations were provided by German/Norwegian MIDAS sounding rocket launches as a part of each rocket sequence.

Sodium density data obtained with the Weber lidar during the two rocket salvos are displayed in the left panels of Figure 1. The right panels show photon counts in three receiver channels (to allow for simultaneous wind and temperature measurements) due to resonance and Rayleigh (top and bottom) backscatter near the mesopause and in the lower atmosphere, respectively. These data reveal that sodium densities in the MLT are both high in altitude and

low in abundance because of 1) a vertical and meridional mean circulation that is GW induced and provides strong upwelling in the upper summer polar mesosphere and 2) sodium atom chemistry and attachment to NLC particles near and below the mesopause that prevents their resonant absorption and emission. The data on the left also exhibit very large modulations due to GW and tidal activity, with vertical displacements of as much as 4 km peak-to-peak, evidence of overturning of the sodium (and neutral) density profiles, and time scales ranging from ~10 min to 12 hr. Indeed, the sodium density data are a sufficiently good tracer of vertical motions that they were able to be used to describe the spectrum of motions at this altitude (Williams et al., 2004). They also enable studies of the microphysics near the mesopause in concert with other radar, Rayleigh lidar, and rocket measurements of NLC, electron and ion profiles, and polar mesosphere summer echoes (PMSE) that arise from sharp electron gradients caused by particle attachment (She et al., 2005).

Even under summer conditions, with full daylight and minimum sodium densities in the MLT, the Weber lidar made high-resolution measurements of temperature and zonal wind with two beams inclined 20^o east and west of zenith. These data, shown in Figure 2 and averaged for 1 hr, exhibit the potential for precision dynamics studies of small-scale processes in the summer MLT. Also shown in the upper panels are both an adiabatic temperature gradient (-9.5 K/km) and strong positive gradient (40 K/km) for comparison with the measurements. Very large gradients in zonal wind are likewise observed (shown are gradients of 50 and 100 m/s/km) and are among the largest gradients ever observed in this region (Fritts et al., 2004). These gradients are also indicative of unusually large GW amplitudes, wind shears, and the potential for GW instability and turbulence in this environment. Indeed, these and other correlative measurements have enabled us to demonstrate much greater variability near the summer mesopause than has been seen (or anticipated) in the past, a link between large-scale and small-scale wave motions, and a degree of inter-hemispheric coupling that was unexpected and surprised many researchers (Goldberg et al., 2004; Fritts et al., 2004; Rapp et al., 2004).

A detailed comparison of temperature measurements with the Weber lidar and the CONE ionization gauge flown on the MIDAS sounding rockets was performed and is shown in Figure 3. In this case, lidar data were averaged for 1 hr and 500 m, and error bars show uncertainties due to photon statistics. The two measurements agree extremely well above the mesopause (~ 89 km), below which there is very little free sodium (She et al., 2004), and appear to validate both measurement techniques. Differences in temperatures and gradients at higher altitudes are likely indicative of the strong, and highly spatially variable, GW activity in this region, which experiences strong increases in vertical gradients of wind and temperature in the highly stratified lower thermosphere (Fritts et al., 2004).

CONE and other ground-based and in situ data collected during the summer rocket campaign also provided correlative data on the GW motions, gradients, and propagation at lower altitudes that helped us to understand and quantify MLT dynamics more completely. An example of our analysis of balloon and falling sphere data that allowed us to estimate GW phase speeds and propagation directions is shown in Figure 4 (Schoech et al., 2004; Williams et al., 2004). These data confirmed that the GW spectrum acquires increasing anisotropy in propagation direction with altitude because of the filtering of the spectrum, and removal of those GWs approaching critical levels, due to mean wind shears. These and other results were reported in a series of

eight papers arising from the summer MaCWAVE/MIDAS campaign in a special issue of GRL in December 2004.

At higher altitudes, CONE and falling sphere data supported the claim made above based on Weber lidar data that the summer mesopause was unusually dynamically active, with larger than normal GW amplitudes, shears, and instabilities. Shown in Figures 5 and 6 are plots of GW temperature variances obtained with falling sphere data and turbulence intensities derived with CONE high-resolution data. First, the falling sphere temperature variances during 2002 were significantly larger than a "typical" summer profile at altitudes above ~75 km and support the claim of larger GW amplitudes and shears in 2002 based on Weber lidar measurements at higher altitudes (Rapp et al., 2004). Turbulence estimates (energy dissipation rates) shown in Figure 6 likewise depart from previous summer mesopause measurements, but even more dramatically. The black line in each panel shows the mean of previous turbulence estimates with CONE or similar instrumentation. Remarkably, the GW activity in the upper mesosphere during summer 2002 was sufficiently strong that significant turbulence intensities were observed to extend a full 10 km lower than ever before observed – with any in situ instruments (Rapp et al., 2004)! These enhanced turbulence levels are also seen to coincide in altitude with a temperature structure that is both more highly stratified than normal and much more structured than normal, with significant positive and negative (adiabatic or greater negative) gradients below the mesopause (see Figure 3 and Rapp et al., 2004). These measurements also reinforce the statements made above based on Weber lidar measurements above the mesopause. Indeed, the larger GW amplitudes that occurred in the upper mesosphere in July 2002 were a consequence of the larger than normal stability of the mean environment and themselves enabled the larger GW amplitudes and shears occurring at higher altitudes (Fritts et al., 2004).

The various data sets described above all appeared to have a common dynamical link. This link was an apparently surprisingly different mean mesopause thermal and wind structure than was typical of polar summer mesopause conditions. However, it was not clear immediately why this was the case. The various components of the mean summer mesopause environment are shown for reference in Figure 7. In each panel, the mean structure observed during 2002 is shown in red, with "typical" or previous annual means shown in blue, green, or black. The point to be made here is that all fields, temperature, zonal wind, and meridional wind, were significantly different than normal in summer 2002. The differences were also linked dynamically and suggested a common cause. GWs provide the primary forcing of the summer mesopause, driving a meridional and vertical mean circulation (the residual, or GW-driven, circulation) that forces the southward jet near the mesopause and (via continuity) the vertical motion that lifts sodium atoms and cools the upper mesosphere. But 2002 had a different structure in important ways. The mean meridional (southward) circulation was stronger at lower altitudes (~70 – 75 km) and weaker near the mesopause than in previous years (see Figure 8). This caused more upwelling and colder mean temperatures at lower altitudes (see the upper panels in Figure 7), but smaller upwelling and warmer temperatures near the mesopause. The result was a more positive (less negative) mean temperature gradient, high mean stability, and a greater ability to support GW motions in the upper mesosphere than in a normal year (when near-adiabatic mean temperatures strongly suppress GW amplitudes). The link of these temperature and residual circulation changes was not recognized immediately. But Becker et

al. (2004, GRL MaCWAVE/MIDAS special issue) showed how all of these changes could arise as a result of stronger than normal planetary wave activity in the southern hemisphere in winter and altered inter-hemispheric GW forcing (see Figure 9, Goldberg et al., 2004). These results were later confirmed in a more comprehensive study of the same dynamics by Becker and Fritts (2006). Thus, Weber lidar, and related in situ and ground-based, measurements at a polar latitude in summer made a striking contribution to our knowledge of mean state, GW, and turbulence variability, and to the potential for inter-hemispheric coupling that was not anticipated or appreciated previously. Indeed, these data and the associated analyses have made significant contributions in all of the areas highlighted in our four initial Research Objectives listed above.

2. Dynamics of the winter polar atmosphere

Following the successful 2002 summer MaCWAVE/MIDAS rocket program, we then attempted to quantify mountain wave excitation, upward propagation, and MLTI effects, including momentum flux divergence, mean flow forcing, and wave instability, interactions, and turbulence generation under winter conditions. This was done using correlative rocket, ground-based, and balloon measurements from ESRANGE, ARR, and ALOMAR (northern Scandinavia is a preferred site for such MLTI penetration of mountain waves, see below). These measurements were further enhanced by TIMED SABER temperature measurements. Thus, as for the summer program, these correlative data comprise the most comprehensive data set for polar winter dynamics studies in the MLT that has ever been assembled.

At each site, key correlative data were collected using the comprehensive ground-based lidar and radar measurement capabilities of ALOMAR along with radiosonde measurements of wave structures at tropospheric and stratospheric altitudes. Additional ground-based measurements at ESRANGE and aircraft measurements of winds, temperatures, and wave structures also contributed correlative data of value to the winter campaign.

Like the summer program, the MaCWAVE winter measurement program was also very successful, though for reasons we had not anticipated. We had hoped to capture mountain wave penetration to both lower and very high altitudes with the two rocket sequences. Because of a stratospheric warming, however, we were able to achieve sensitivity to only the lower altitude penetration of mountain waves, their penetration to higher altitudes being blocked by critical levels in the mean winds. Indeed, our characterization of GW blocking and critical level filtering (see Figure 10) is the most striking demonstration of these dynamics of which we are aware at any site (Wang et al., 2006).

We were also successful in capturing a very large wave event during the second salvo at a time when correlative data were obtained at both ALOMAR and ESRANGE employing radar and lidar instrumentation at both sites because of fortuitous clear skies. This has proven to be primarily a manifestation of an especially large semidiurnal tide, with coherent wind and temperature fields at ESRANGE and ALOMAR with superposed higher-frequency gravity wave activity. An example of the correlative data obtained with the Weber sodium lidar at ALOMAR accompanying the second winter rocket sequence at ESRANGRE is shown in the left panels of Figure 11. Shown are 15-min and 1-km averages of temperature (top), zonal wind

(middle), and sodium density (bottom). These fields all exhibit both large-amplitude semidiurnal tidal structures and high-frequency GWs (see the altitude traces of temperature in the right panels). The variations in tidal amplitude and period over six days around this interval employing both Weber lidar and meteor radar data are shown in Figure 12. A merged temperature field compiled from data from multiple instruments during the MaCWAVE winter campaign (see Figure 13) has provided a comprehensive view of the large- and small-scale motions throughout the atmosphere (Williams et al., 2006a). An analysis of the airglow data obtained from ESRANGE revealed a variety of motions ranging from GWs having largely verticall propagating character (in contrast to many previous observations) as well as evidence of significant relatively large-scale instability structures accompanying the strong tidal shears (Nielson et al., 2006), the measured phase structures of which are shown at two times in Figure 14. The analyses surveyed here are now in press in a special MaCWAVE issue of Ann. Geophys.

Other winter dynamics contributions include our participation in measurements and analyses accompanying the Japanese Dynamics and Energetics of the Lower Thermosphere during Aurora (DELTA) rocket campaign at ARR and ALOMAR in December 2004 and individual measurements with the Weber lidar of GW momentum fluxes at several other times allowing relatively continuous data sets. As the name suggests, the objective of the DELTA campaign was to investigate the response of lower thermospheric dynamics and energetics to auroral energy input. Measurements with the Weber lidar during the DELTA campaign revealed an unusual GW structure which appeared to have a well-defined vertical structure and a very large vertical velocity, suggesting in situ generation (Williams et al., 2006b). This structure is shown in Figure 15, has not been fully explained at present, and remains the subject of further study.

Finally, momentum flux measurements are surely among the most important and challenging measurements related to GW effects in the MLT. A series of such measurements, however, demonstrated that the Weber lidar can perform such assessments on relatively short time scales (i.e. with high measurement confidence) and revealed a familiar anti-correlation of the major momentum flux contributions with the large-scale wind field accounting for GW filtering (Williams et al., 2006c). Examples of these data and the mean and 2-hr estimates of zonal winds and momentum fluxes computed from them are shown in Figures 16 to 18. Note, both in the mean profiles and in the 2-hr profiles having larger winds or momentum fluxes, a tendency for an anti-correlation between these two quantities that is largely consistent with observations at a number of other sites at lower altitudes. Such measurements have also been performed on several occasions more recently. Only the Weber lidar, however, has the ability at present to make such measurements with high spatial and temporal resolution extending into the lower thermosphere.

3. Related theoretical studies

While the large majority of resources were devoted to Weber lidar measurements and analyses of lidar and correlative data, we also employed a much smaller fraction of resources for partial support of theoretical efforts judged to be relevant to AFOSR needs. Modeling efforts employing a Fourier-Laplace method addressed upward penetration of GWs arising from deep tropical convection and helped to motivate two field programs to study GW seeding of

equatorial spread-F and sprites as an intended collaboration with the Air Force C/NOFS satellite, scheduled for launch in 2005. The satellite has yet to be launched, but our field measurements were successful, and those analyses are proceeding under separate funding. We also recently performed a new (and complete) derivation of the viscous dispersion relation for GWs penetrating to high altitudes. This was never done until now, and our effort, we believe, represents a new means of quantifying GW effects well into the thermosphere under solar minimum and solar maximum conditions (Vadas and Fritts, 2005, 2006).

Appendix A: In-house Activities

Instructions: Provide all information identified below for the last FY only. "Personnel" should include each scientist or engineer who contributed to the research during the year. Publication of articles derived from the research should be listed chronologically in bibliography format. Attach reprints. List only invention disclosures derived from this specific research effort. Honors may include recognition both inside and outside the academic and Air Force science & technology (S&T) communities. Extended scientific visits may include collaboration with other research programs, both foreign and US.

Personnel:

	Name	Degree	Discipline	Involvement
In House Employees	Dave Fritts	Ph.D.	Physics	1 mo/yr
	Biff Williams	Ph.D.	Physics	2 mo/yr
Subcontract Personnel:				
	C.-Y. She	Ph.D.	Physics	1 mo/yr
	Joe Vance	Ph.D.	Physics	1 mo/yr
	Kam Arnold	undergrad.	Physics	travel only
	Phil Acott	undergrad.	Physics	travel only

Publications Citing this AFOSR Support (current and anticipated):

1. Becker, E., and D. C. Fritts, 2006: Interhemispheric coupling by the residual circulation: Enhanced gravity-wave activity and interhemispheric coupling during the McWAVE/MIDAS northern summer program 2002, *J. Atmos. Solar-Terres. Phys*., MaCWAVE special issue, in press.

2. Fritts, D. C., S. L. Vadas, K. Wan, and J. A. Werne, 2006: Mean and Variable Forcing of the Middle Atmosphere by Gravity Waves, *J. Atmos. Solar-Terres. Phys.,* in press.

3. Fritts, D. C., B. Williams, C.-Y. She, J. Vance, M. Rapp, F.-J. Luebken, F. J. Schmidlin, A. Muellemann, and R. A. Goldberg, 2004: Measurements and implications of extreme gradients of wind and temperature near the summer mesopause during the summer MaCWAVE/MIDAS rocket campaign, *Geophys. Res. Lett.*, **31**, doi:10.1029/2003GL019389.

4. Goldberg, R. A., D. C. Fritts, B. P. Williams, F.-J. Luebken, M. Rapp, W. Singer, R. Latteck, P. Hoffmann, A. Muellemann, G. Baumgarten, F. J. Schmidlin, C.-Y. She, and D. A. Krueger, 2004: The MaCWAVE/MIDAS rocket and ground-based measurements of polar summer dynamics: Overview and mean state structure, *Geophys. Res. Lett.*, **31**, doi:10.1029/GL2004GL019411.

5. Goldberg, R. A., D. C. Fritts, B. P. Williams, W. Singer, R. Latteck, P. Hoffmann, G. Baumgarten, F. J. Schmidlin, and C. Y. She, 2006: The MaCWAVE program to study gravity wave influences on the polar mesosphere, *Ann. Geophys*., in press.

6. Nielson, K., M. J. Taylor, P.-D. Pautet, N. Mitchell, C. Beldon, W. Singer, D. C. Fritts, F. J. Schmidlin, and R. A. Goldberg, 2006: Propagation and ducting of short-period gravity waves at high latitudes during the MaCWAVE winter campaign, *Ann. Geophys.*, in press.

7. She, C. Y., B. P. Williams, P. Hoffmann, R. Latteck, G. Baumgarten, J. D. Vance, J. Fiedler, P. Acott, D. C. Fritts, U. von Zahn, F.-J. Luebken, 2005: Observation of anti-correlation between sodium atoms and PMSE/NLC in summer mesopause at ALOMAR, Norway (69N, 12E), *J. Atmos. Solar-Terres. Phys*., **68**, 93-101, doi:10.1016/j.jastp.2005.08.014.

8. Singer, W., R. Latteck, P. Hoffman, B. Williams, D. C. Fritts, Y. Murayama, and K. Sakanoi, 2005: Tides in the MLT and during the MaCWAVE/MIDAS summer rocket program, *Geophys. Res. Lett.,* **32**, doi:10.1029/2004GL021607.

9. Vadas, S. L., and D. C. Fritts, 2004: Thermospheric responses to gravity waves arising from mesoscale convective complexes, *J. Atmos. Solar Terres. Phys.*, **66**, 781-804.

10. Vadas, S. L., and D. C. Fritts, 2005: Thermospheric responses to gravity waves: Influences of increasing viscosity and thermal diffusivity, *J. Geophys. Res*., **110**, D15103, doi:10.1029/2004JD005574.

11. Vadas, S. L., and D. C. Fritts, 2006: The influence of solar variability on gravity wave dissipation in the thermosphere, *J. Geophys. Res*., in press.

12. Wang, L., D. C. Fritts, B. P. Williams, R. A. Goldberg, and F. J. Schmidlin, 2006: Gravity Waves in the Middle Atmosphere during the MaCWAVE Winter Campaign: Evidence of Mountain Wave Critical Level Encounters, *Ann. Geophys*., in press.

13. Williams, B. P., D. C. Fritts, C. Y. She, G. Baumgarten, and R. A. Goldberg, 2006a: Gravity wave propagation, tidal interaction, and instabilities in the mesosphere and lower thermosphere during the winter 2003 MaCWAVE rocket campaign, *Ann. Geophys*., in press.

14. Williams, B., D. C. Fritts, L. Wang, C.-Y. She, J. Vance, F. J. Schmidlin, R. A. Goldberg, A. Muellemann, and F.-J. Luebken, 2004: Gravity waves in the arctic mesosphere during the MaCWAVE/MIDAS summer rocket, *Geophys. Res. Lett.*, **31**, doi:10.1029/GL2004020049.

15. Williams, B., D. C. Fritts, C.-Y. She, and J. Vance, 2006c: First measurements of gravity wave momentum fluxes with the Weber Na lidar at ALOMAR in northern Norway, *J. Geophys. Res.*, submitted.

16. Williams, B., J. D. Vance, C.-Y. She, D. C. Fritts, T. Abe, and E. Thrane, 2006b: Sodium lidar measurementsof waves and instabilities near the mesopause during the DELTA rocket campaign, *Earth Planets Space*, in press.

Technical Presentations under this Research Support

Fritts, D. C., Mean and variable forcing by gravity waves in the middle atmosphere, Workshop on Coupling in the MTLI System, Bath, U.K., July 2004.

Goldberg, R. A., and D. C. Fritts, MaCWAVE: An experimental program to study gravirt wave forcing of the polar mesosphere and lower thermosphere during summer and winter, Workshop on Coupling in the MTLI System, Bath, U.K., July 2004.

Fritts, D. C., and R. A. Goldberg, The MaCWAVE/MIDAS rocket campaigns: A survey of results, COSPAR, Paris, August, 2004.

She. C. Y., Lidars for Atmospheric Studies, at Notiona MST Radar Facility, Tirupati, India, 2004.

She, C. Y., Meeting challenges of middle atmospheric research with lidar observations, India-US conference on space, application and commerce, Bangalore, India, 2004.

Fritts, D. C., Plans for the NASA Gravity Wave – Equatorial Spread F Seeding Campaign, C/NOFS Workshop, Estes Park, CO, January 2005.

Fritts, D. C., Advanced topics in gravity wave dynamics, a "short course" presented to staff at INPE in preparation for the "Gravity Wave – Equatorial Spread F Seeding Campaign", Sao Paulo, Brazil, June 2005.

Fritts, D. C., Gravity wave propagation and effects extending to high altitudes, IAGA Symposium, Toulouse, July 2005.

Fritts, D. C., Gravity Wave Forcing, Interactions, and Variability in the MLT, invited talk, Fall AGU Meeting, 2005.

Wang, L., D. C. Fritts, et al., Gravity wave propagation and critical level filtering observed during the MaCWAVE winter campaign, Fall AGU Meeting, 2005.

Williams, B. P., D. C. Fritts, C.-Y. She, and J. D. Vance, Measurement of gravity wave momentum fluxes with the Weber sodium lidar at the ALOMAR observatory, Fall AGU Meting, 2005.

Final Report Figures: AFOSR Contract F49620-03-C-0045

D. C. Fritts (PI) and C. Y. She (Co-I)

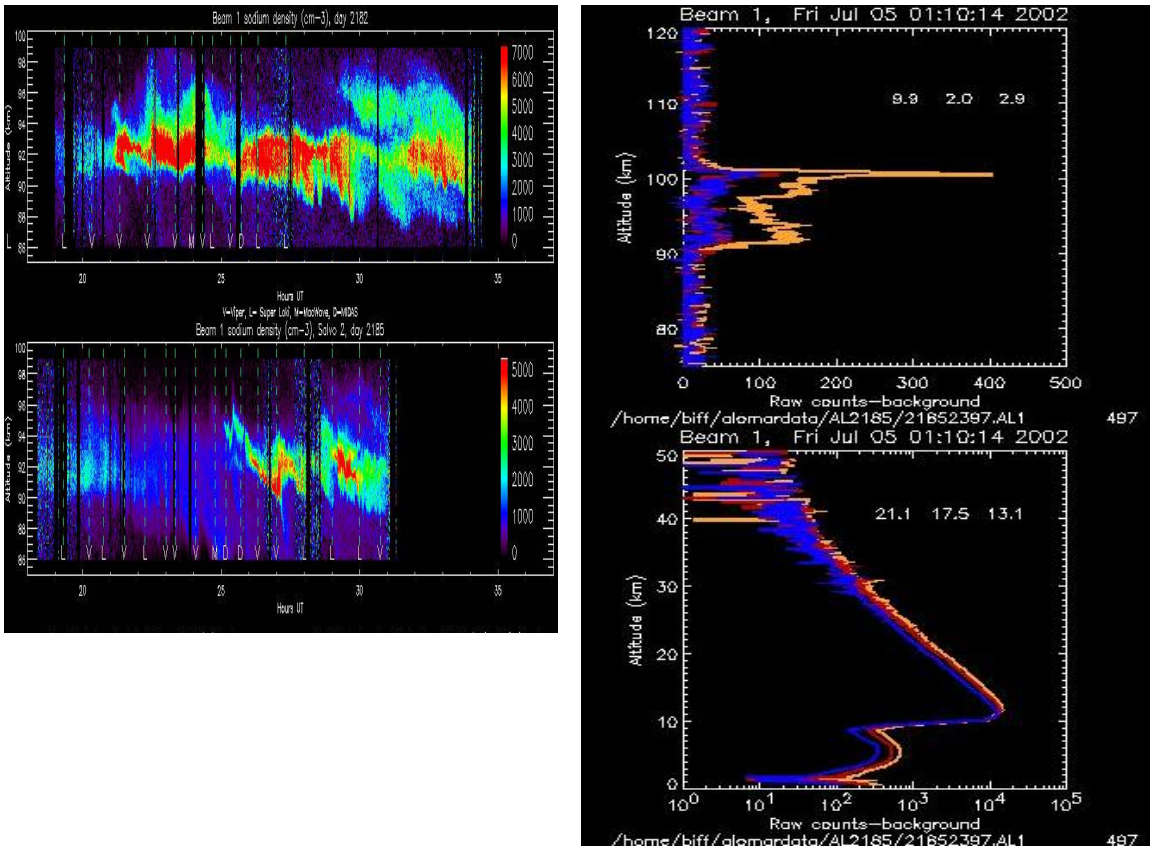

Figure 1. Sodium densities as a function of time during the two summer MaCWAVE/MIDAS rocket salvos (left) and photon counts in the three receiver channels (right) in the lower thermosphere (top) and lower atmosphere (bottom).

Figure 2 (next page). Temperatures (top) and zonal winds (bottom) measured with the east (blue) and west (red) beams of the Weber sodium lidar during the first summer rocket salvo. Data are shown at an altitude resolution of 150 m and averaged for 1 hour about the time of each MET rocket launch from 2020 to 2320 LT. Also shown in all panels are corresponding falling sphere measurements at lower altitudes. Uncertainties due to photon statistics (for the lidar) and vertical smoothing (for the falling spheres) are shown with horizontal errors bars. The dashed lines in the lower panels shown zonal winds measured with the meteor radar at 3-km and 1-hr resolution. The lidar data reveal extreme gradients in both temperature and zonal wind indicative of very strong gravity wave activity during the measurement program (see text for details). Note also that the lidar captures features in the temperature and wind fields that cannot be sensed with falling spheres or ground-based instrumentation.

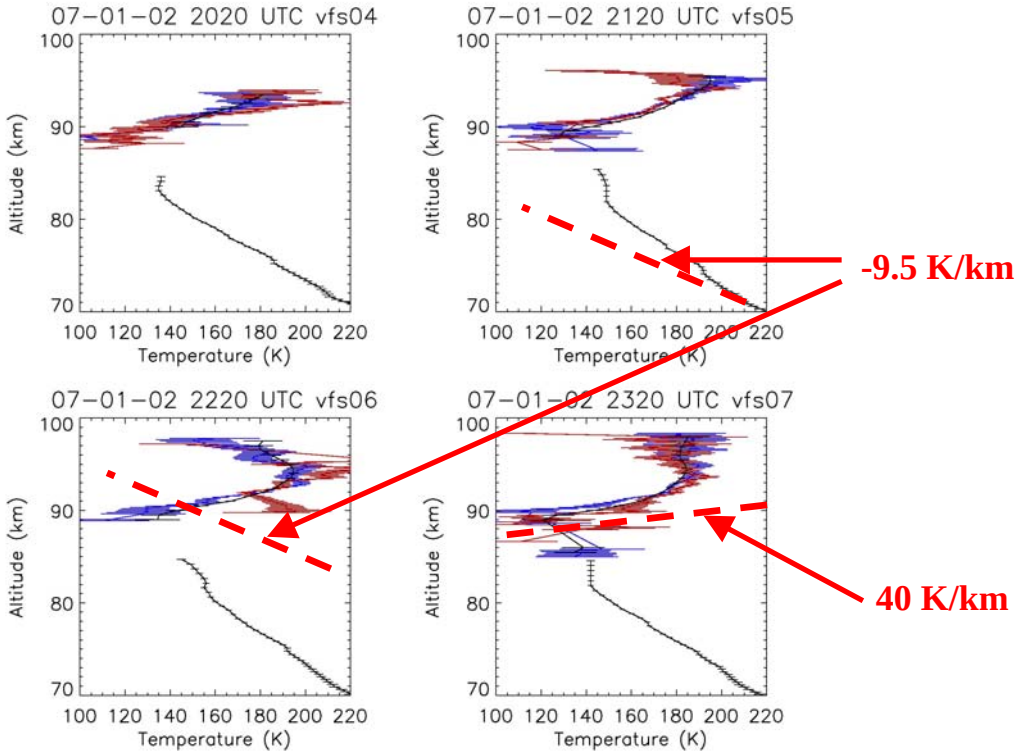
07–01–02 2020 UTC vfs04
07–01–02 2120 UTC vfs05
07–01–02 2220 UTC vfs06
07–01–02 2320 UTC vfs07
Altitude (km)
Temperature (K)
100
90
80
70
100 120 140 160 180 200 220
-9.5 K/km
40 K/km

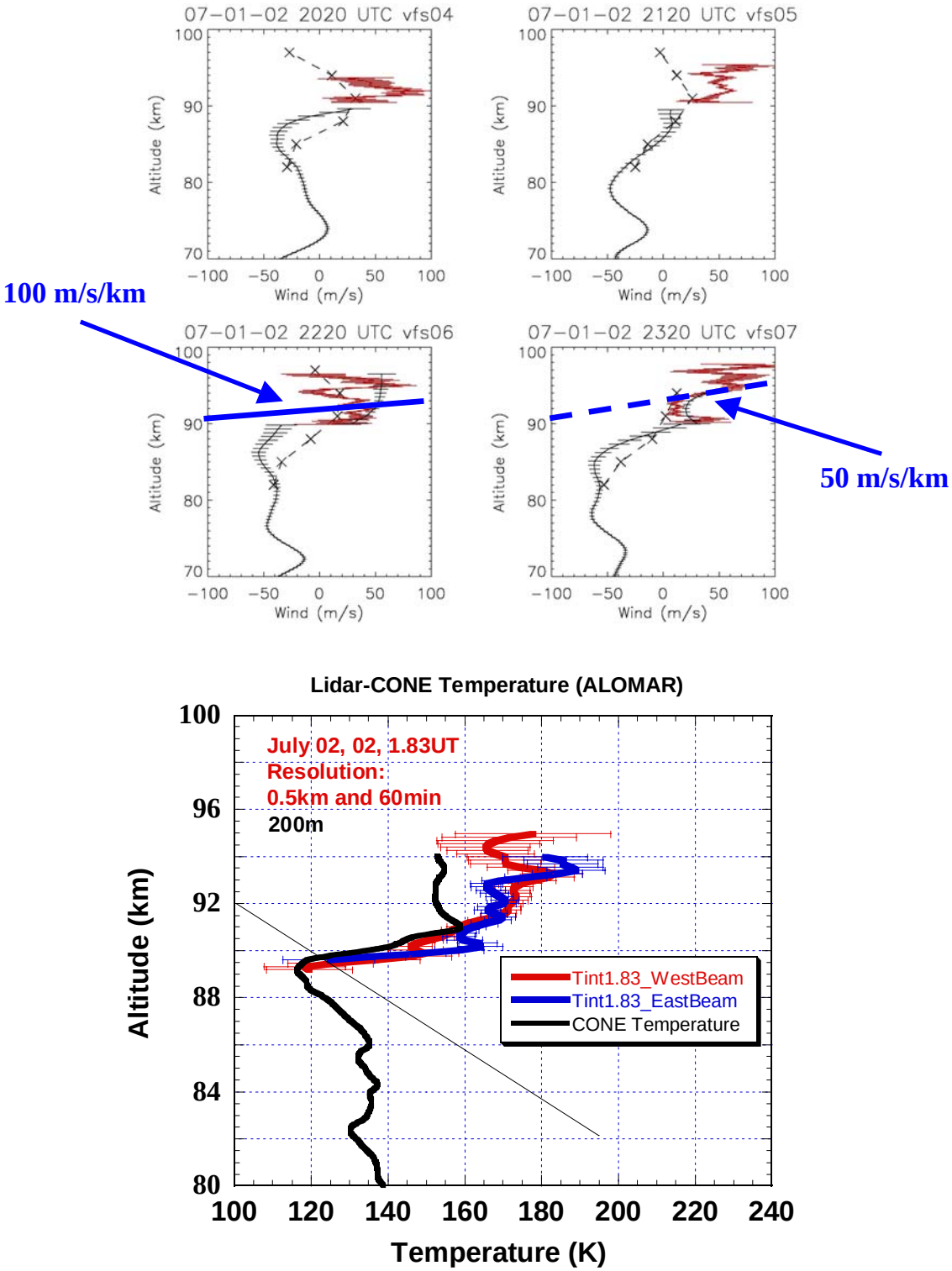

Figure 3. Temperature profiles obtained with the Weber lidar in the east (blue) and west (red) beams and with the CONE ionization gauge aboard the MIDAS rocket during the first summer MaCWAVE/MIDAS salvo. Differences between the profiles are due to different locations in a very dynamically active mesopause gravity wave field. Spacing

between the lidar beams (at 20^{o} zenith angles) was ~60 km and the CONE measurement was ~30 km north of the west lidar beam. Gradients are ~50 K/km for CONE to ~100 K/km for the Weber lidar.

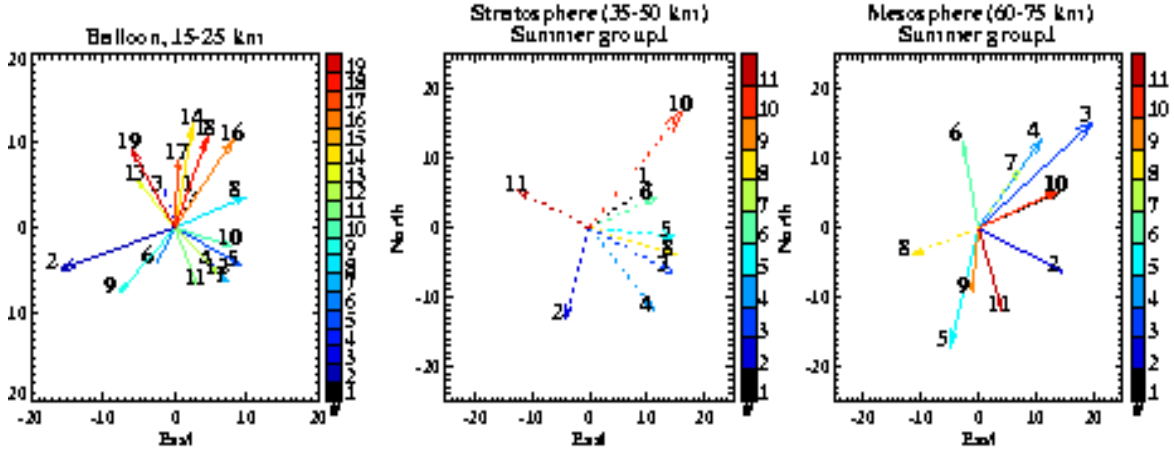

Figure 4. Distributions of propagation direction and horizontal phase speed for gravity waves inferred from a hodograph analysis of balloon and falling sphere data during the summer MaCWAVE salvoes. The trend is toward an increasing eastward propagation bias with increasing altitude, consistent with expectations of filtering theory.

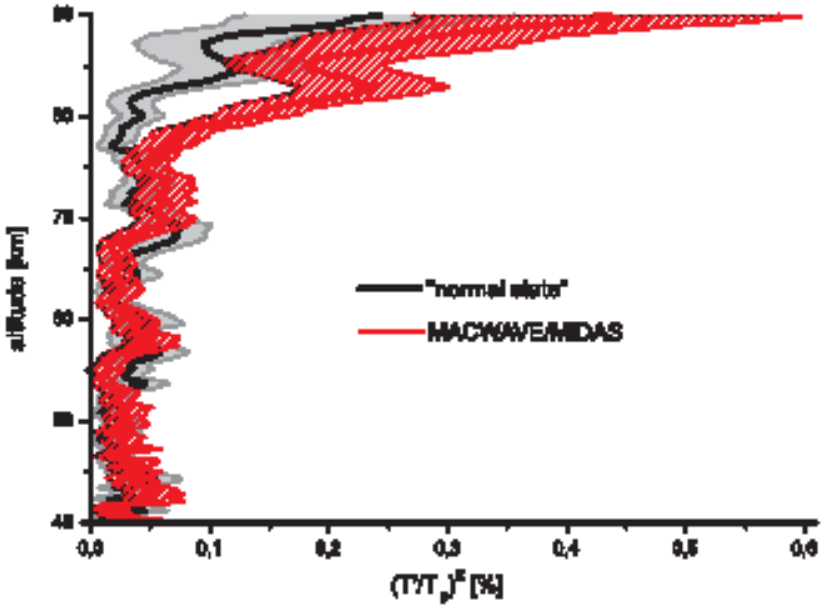

Figure 5. Temperature variances and 1-sigma standard deviations obtained from falling sphere measurements comparing summer 2002 (red) with previous "typical" (black and grey) measurements. Variances were statistically larger above ~75 km in 2002.

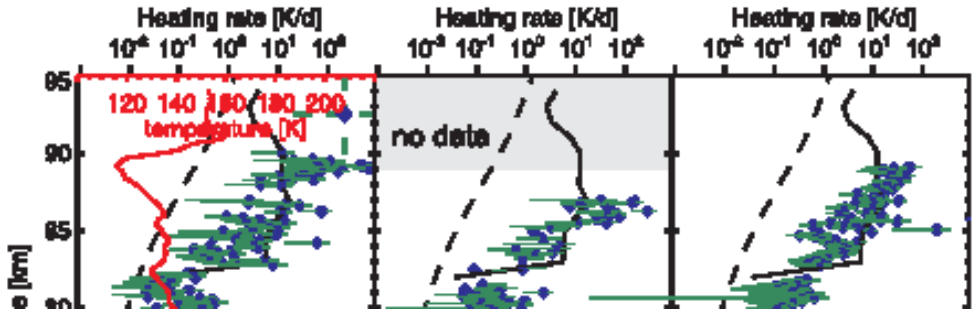

Figure 6. Estimates of turbulence intensities (energy dissipation rate, ε) (blue) and uncertainties (green) obtained with the CONE instrument aboard the MIDAS sounding rockets during the summer 2002 MaCWAVE/MIDAS rocket campaign. Black lines show the mean of previous polar summer measurements. The red line in the left panel shows the CONE temperature profile for reference (from Rapp et al., 2004). Vertical resolution with the CONE instrument is ~100 m.

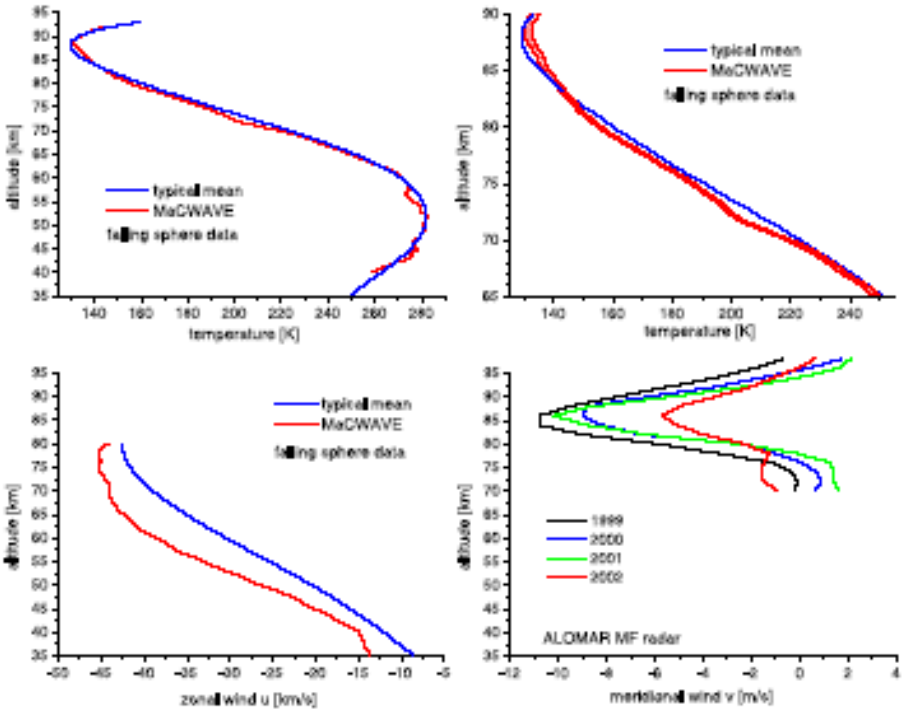

Figure 7. MaCWAVE/MIDAS measurements (red) compared with "typical mean" (blue) or other single-year means (black, blue, green, at lower right). Panels show mean temperature over a large altitude range (upper left), a closer view of mean temperature in the MLT (upper right), zonal wind (lower left), and meridional wind (lower right).

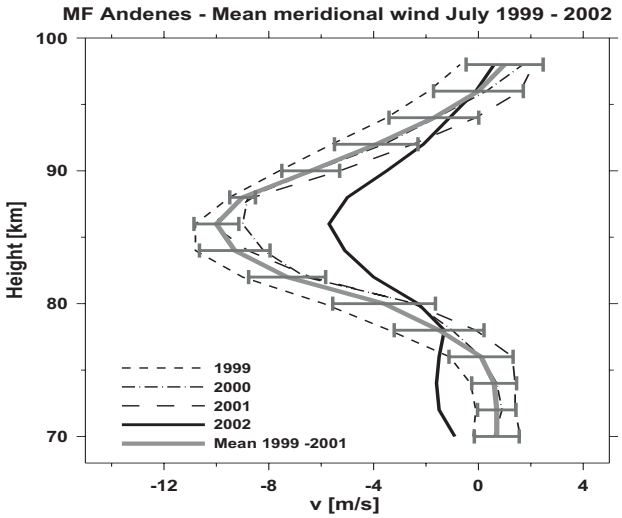

Figure 8. A second view of the mean meridional winds during July 2002 compared the average of the three previous years that emphasizes stronger (weaker) southward flow at lower (higher) altitudes in 2002.

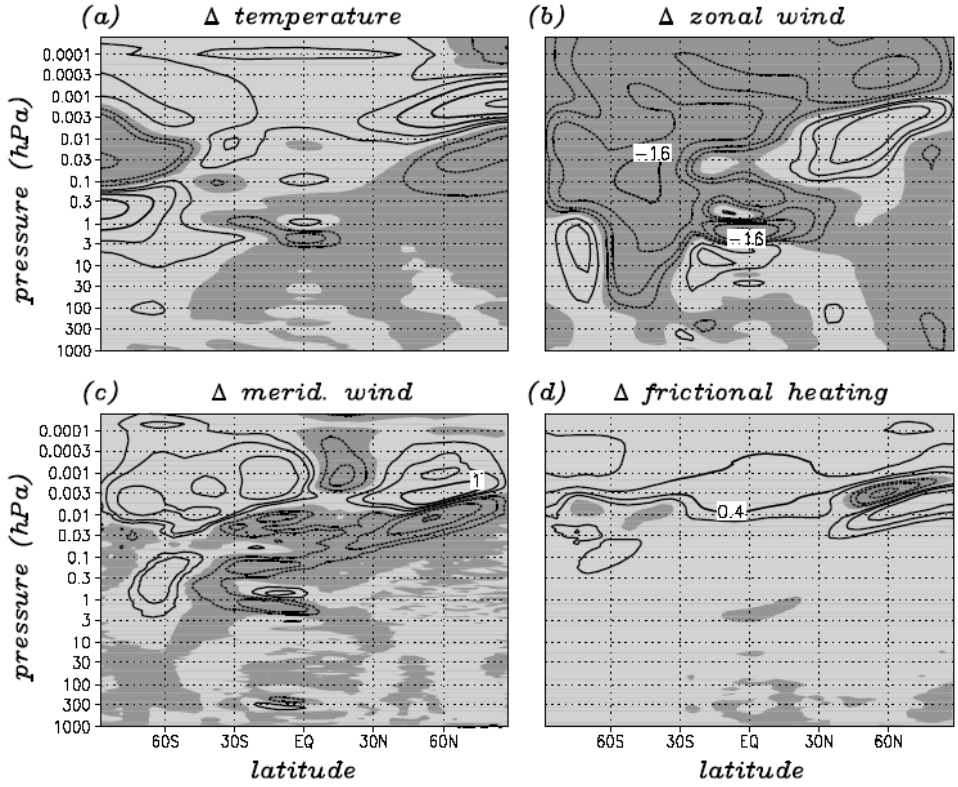

Figure 9. Zonal-mean differences between "summer 2002" and a "normal July" as simulated by Becker and Fritts (2006). Differences are largely consistent with summer MaCWAVE observations, and they arise because of enhanced southern hemisphere planetary wave activity and associated changed in the GW forcing in both hemispheres.

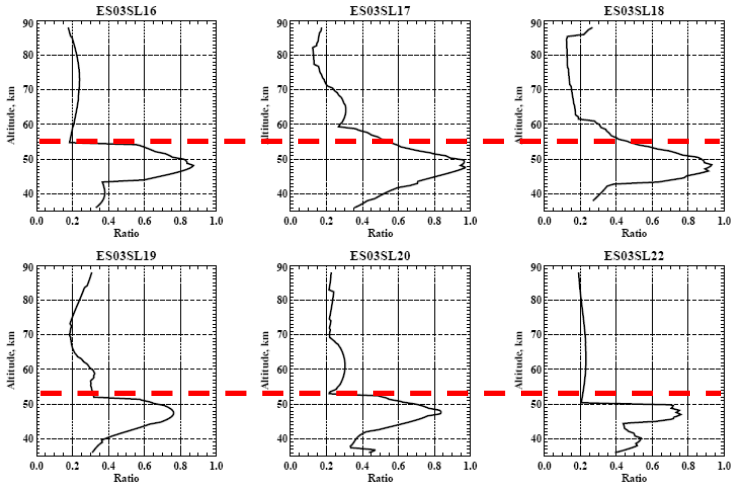

Figure 10. GW amplitudes measured relative to intrinsic frequency, u'/(c – U), for hourly falling sphere measurements during the winter MaCWAVE rocket campaign. The sharp increases below the dashed red lines and the decreases above are striking indications of critical level filtering. The dashed red lines show the approximate critical level positions based on GW propagation directions (Wang et al., 2006).

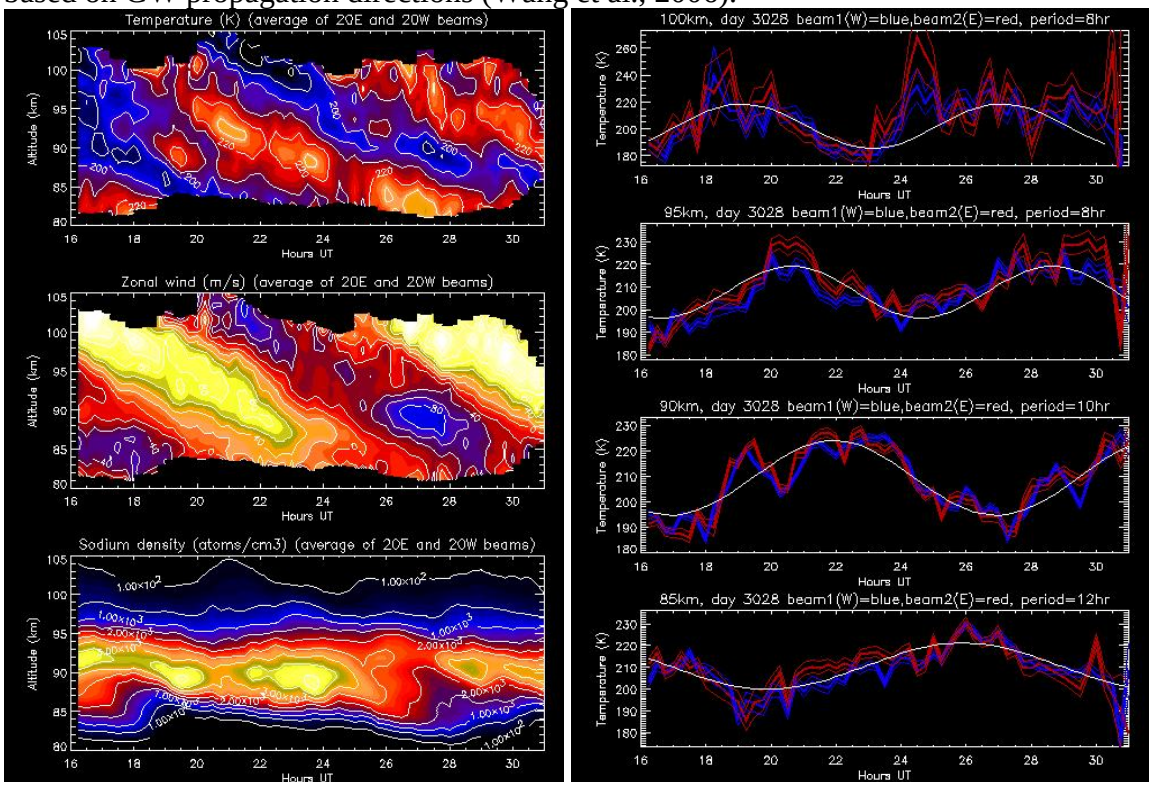

Figure 11. Sodium lidar measurements of temperature, zonal wind, and sodium density (top to bottom, right) at ALOMAR accompanying the large semidiurnal tide captured with the second winter rocket sequence at ESRANGE. Temperatures at specific altitudes at shown in the panels on the right. These and other data suggest a highly dynamically active environment during this interval.

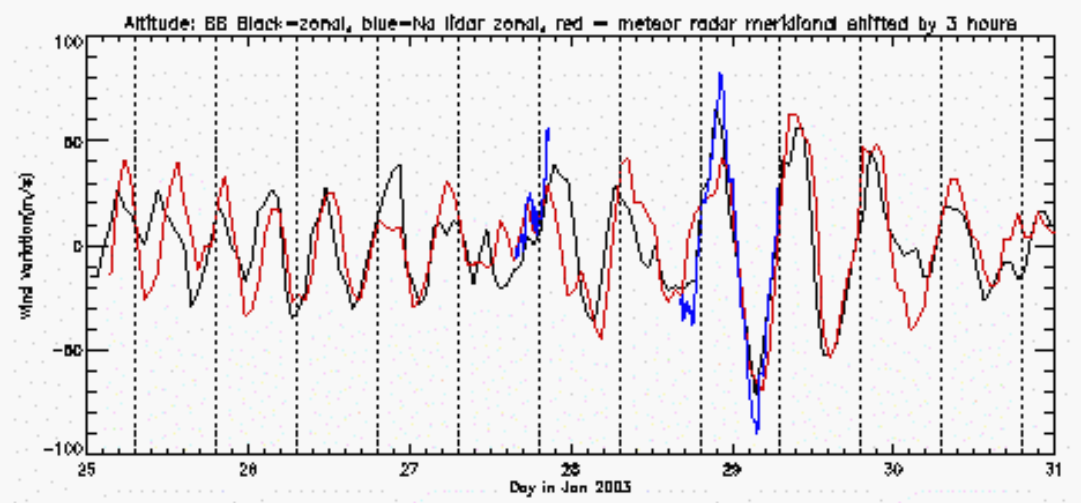

Figure 12. Hourly winds obtained with the Weber lidar (blue, zonal) and meteor radar (red and black, with meridional advanced by 3 hours for phase comparison) during the MaCWAVE first winter salvo. The variations show a clear terdiurnal tide at early times, replaced thereafter by a large-amplitude semi-diurnal motion (Singer et al., 2005).

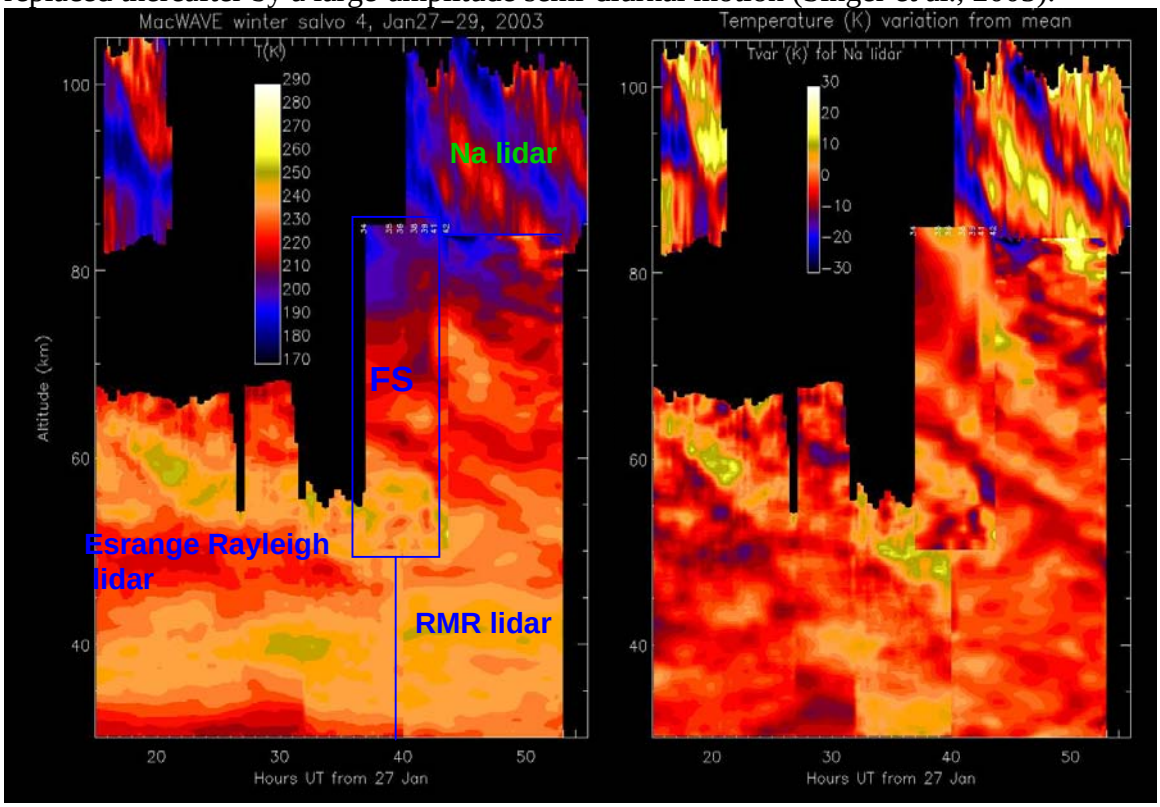

Figure 13. Merged total (left) and perturbation (right) temperature measurements including the Weber lidar (upper altitudes), the Esrange and ALOMAR (RMR) Rayleigh lidars (lower altitudes), and falling spheres (intermediate altitudes) during the second

winter MaCWAVE rocket salvo. Note the clear phase descent of all wave motions and the variations in spatial and temporal scales with altitude.

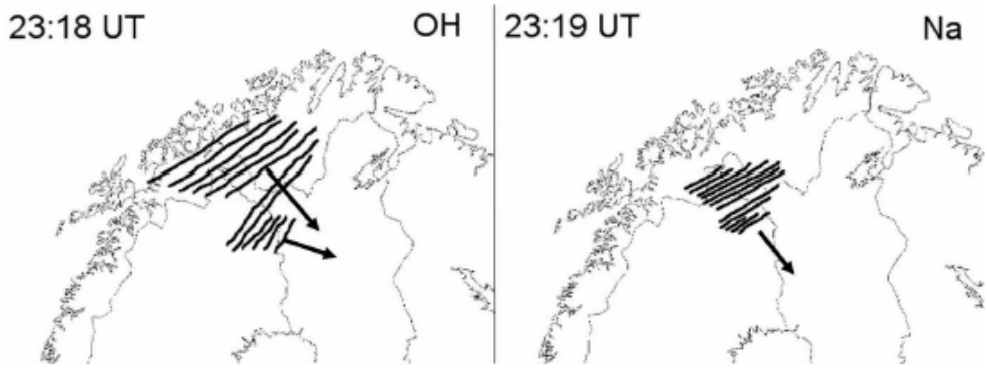

Figure 14. Instability structure alignments inferred in OH and Na airglow measurements at ESRANGE at a time of strong wind shear. Analysis suggests these were a signature of Kelvin-Helmholtz shear instability at two different altitudes (Nielson et al., 2006).

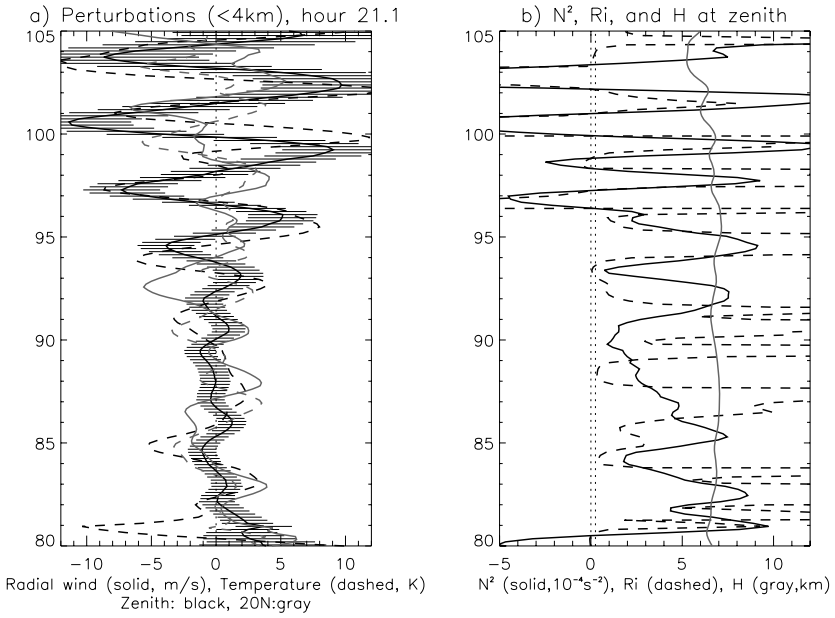

Figure 15. Large vertical wind perturbations (left, solid black line with error bars) at 21.0 to 21.2 UT for vertical scales less than 4 km measured with the Weber lidar during the DELTA rocket campaign at ARR in December 2004 (Williams et al., 2006b). The dashed black line in the left panel is the corresponding temperature perturbation in the vertical beam. Grey solid and dashed lines are the radial velocity and temperature in the beam inclined 20^o N for comparison. The right panel displays N^2, the Richardson number (dashed), and the local scale height, H (solid, ~7 km) over this same interval.

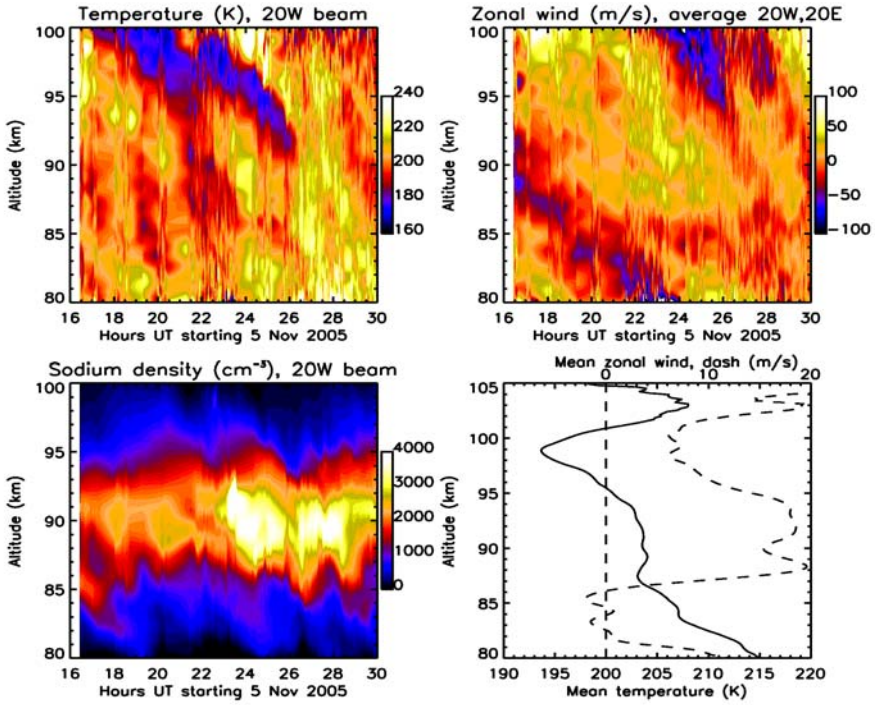

Figure 16. Contours of temperature, zonal wind, and sodium density, and profiles of the zonal mean wind and temperature for a 14-hr observation on 5-6 November 2005.

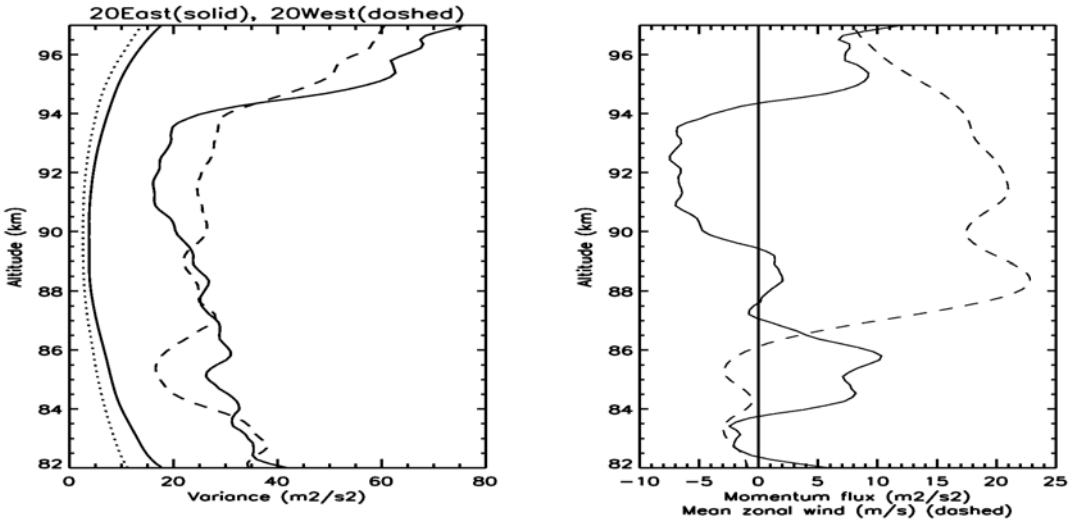

Figure 17. East (solid) and west (dashed) beam radial velocity variances (larger values) and photon noise variances for 5-6 November 2005 using the entire 14-hr data set (left). The right panel shows the overall mean wind (dashed) and momentum flux (solid) computed from the radial beam variances. Note the clear anti-correlation on the right.

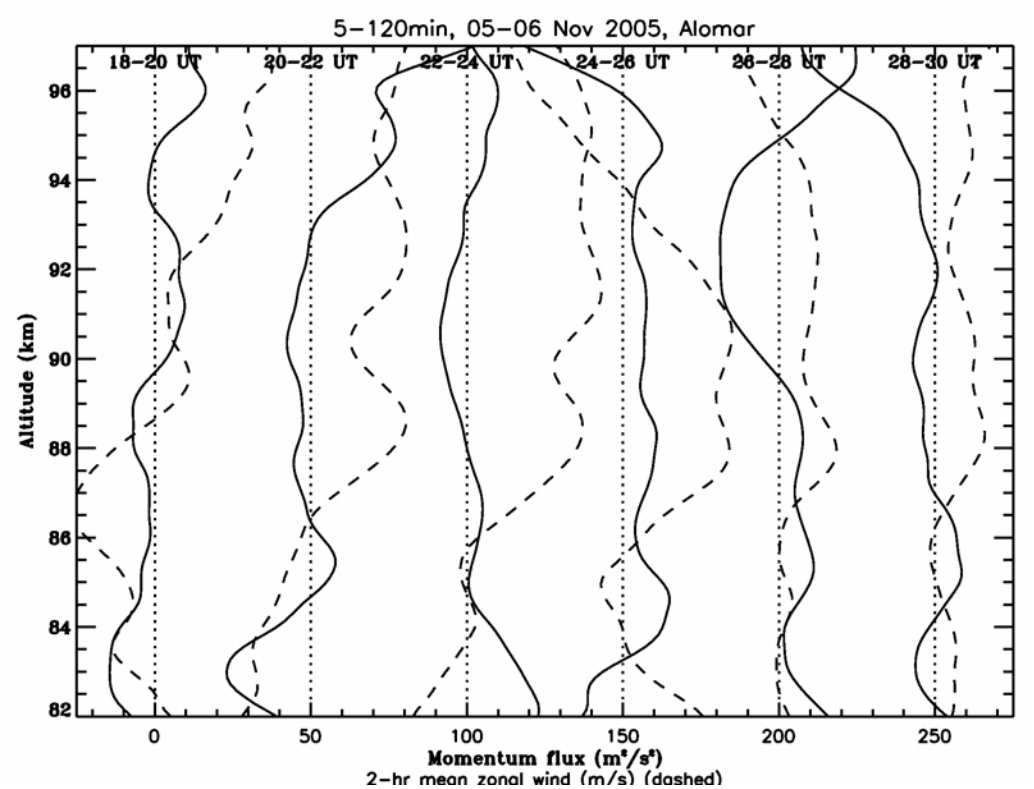

Figure 18. Zonal wind (dashed) and momentum flux (solid) profiles in six 2-hr intervals during the observation on 5-6 November 2005. Note the tendency for anti-correlations to persist for shorter intervals when mean winds and momentum fluxes are large.